Marsh Restoration: Ribbed Mussels (Geukensia demissa) as a Revival Mechanism to Rebuild the Coastal Salt Marshes of Long Island, New York

Andrew J Brinton (andrewbrinton1@gmail.com)
Hofstra University https://orcid.org/0000-0001-8373-4146

Research Article

Keywords: Marshes, Long Island, Restoration, Remediation, Ribbed Mussel, Spartina

Posted Date: August 2nd, 2021

DOI: https://doi.org/10.21203/rs.3.rs-359936/v1

Abstract

Hurricane severity and frequency have been exacerbated by 190 years of anthropogenic climate change. In 2012, Superstorm Sandy decimated Long Island, a 190-kilometer-long island in southeast New York, with up to 4 meters of saltwater inundation due to storm surge, resulting in the highest levels of destruction since the 1938 “Long Island Express.” Sandy was the fifth most costly hurricane on record, after Katrina in 2005, and Harvey, Maria, and Irma in 2017.

Synthetic storm-surge barriers such as concrete-and-steel tidal gates are exorbitantly costly to construct and decrease biodiversity by barring habitat expansion. Natural storm barriers, termed “living shorelines,” have recently been suggested as an alternative, owing to their structurally resilient and regenerative properties. Coastal marshes, one type of natural barrier, are key to holding back storm surge; however, the contiguous United States lost coastal wetlands at 0.15 percent per year from 1998 through 2009, the final year for which the data were available.

This study investigated ribbed mussels (*Geukensia demissa*) as a potential regenerative component of living shorelines. Transects and environmental energetic measurements were applied to draw conclusions between mussel abundance and scarcity and coastline erosion in the waters off Freeport, Long Island. It was discerned that the current rate of marsh disintegration on Long Island is 6.5 to 20 times greater than the national rate, as last measured a decade ago, and certain Long Island regions are projected to lose all coastal wetlands by 2079.

Introduction

Storm surges that result from extreme weather tear apart coastal communities. While the physical damage to homes and businesses may be repairable, thousands of people face lasting trauma, including financial instability, mental anguish, and illnesses caused by high levels of stress. Superstorm Sandy, which struck Long Island, New York, on October 29, 2012, resulted in untold levels of damage, both physical and mental. It caused roughly 65 billion dollars in damage to states along the Eastern Seaboard, in particular New Jersey and New York. The storm, the fifth most destructive on record, wreaked havoc on upward of 650 thousand houses along the coast, and left 8 million homes without power (Newsday, 2012; Federal Emergency Management Agency, 2012).

Humans are fueling the current climate-change crisis by releasing greenhouse gases such as carbon dioxide (Solomon, 2009), methane (Jain, 2003), and nitrogen oxide (Kroeze, 1992) through factories, power plants, and gasoline-powered automobiles, as well as the burning of forest to clear land for agriculture. The accumulation of the compounds in the atmosphere causes the “greenhouse effect” across the world, whereby the “radiative balance” of the Earth is altered. In the past, sunlight passed through the atmosphere, was absorbed by surfaces around the globe, and then reradiated back as infrared heat. Part of that infrared heat was trapped by the atmosphere, and part of it escaped into space. That natural process remains in place. Today, however, rising levels of CO_2, CH_4 and NOx are trapping

greater amounts of infrared heat, warming the Earth, including the oceans, at an accelerating rate (Bowman, 1990; EPA, 2018). In turn, land-based ice in Greenland and Antarctica is melting at an increasing rate, raising sea levels, causing shoreline submergence around the globe. Conservative estimates project that sea level will increase by 65 centimeters by the end of the 21st century (Chaisson, 2018).

Unless human behavior is modified, it is expected that the Earth will reach 500 parts per million of CO_2 in the atmosphere within the next 50 years, after which the planet will reach a potentially untenable "tipping point," when the Earth will continue warming indefinitely and uncontrollably (Jones, 2017).

Climate change played a role in the development of Superstorm Sandy, among other storms, due to the widespread warming of ocean waters along the coast (Brandon et al., 2014). The warmer waters and atmosphere increased the storm's ability to sustain itself and grow, and physical damage was especially injurious to the coasts owing to the storm surge that Superstorm Sandy caused. The abnormally large storm, both in height and width, resulted in surge that lasted longer than predicted, reaching over 3.4 meters above sea level, and 1.2 meters above predicted surge height (Brandon et al., 2014). In addition, the surge was even larger when Superstorm Sandy hit Long Island, New York, due to the storm's landfall on the evening of October 29th, a time of full moon. The exact time of landfall was during high tide. While humans cannot control the tides, it is possible to control their response to calamitous events like Superstorm Sandy. The storm surges from Sandy were unavoidable, but their impact on coastal communities could have been reduced, even prevented, if saltwater marshes had been better preserved (Colle et al., 2008; Cochran et al., 2018) and were intact to 19th century levels.

Salt marshes are resilient, yet fragile environments that sit precariously between the ocean and mainland surrounding the bays and estuaries, and act as bridges from the ocean to the mainland. They are shields and sponges, both absorbing water and acting as walls against storm surge (Cochran et al., 2018). Within marsh communities exist thousands of species of fauna, flora, and microorganisms that aid wetland growth (Gedan et al., 2008).

In the past 50 years, salt marshes along the Atlantic Coast have degraded by 50 to 70 percent (Cochran et al., 2018), depending on the state. Their decline can be attributed to a multitude of chemical and physical threats, which not only shrink the size of the marshes horizontally and vertically, but also poison remaining life forms (Town of Hempstead, 2012).

Nitrogen runoff from urban and suburban development has taken an outsized toll on marsh life. Nitrogen from synthetic fertilizers and chemical waste seeps into streams, bays and mudflats, leading to eutrophication, or nutrient over-enrichment of the environment, which causes mass algal blooms (South Shore Estuary Reserve Council, 2016; Wallace and Baumann, 2014). This, in turn, causes the root structures of "mother species" such as *Spartina alterniflora* and *Spartina patens* to lose a steady oxygen supply due to the overpopulation of oxygen-consuming bacteria and algae. The asphyxiation of the *Spartina* grass shrinks and kills the roots and eventually the entire individual (Bilkovic et al., 2017).

Widespread, this results in a significant loss of sediment retainment within *Spartina* environments, and much of the sediment that would be held together by *Spartina* grasses is lost to the tides.

Inundation and submergence are other factors that cause significant damage to the *Spartina* salt marshes. Inundation is the flooding of marshes that occurs in addition to tidal patterns. Submergence is the physical covering of marshes, whereby the grasses and all life forms held within are submerged (Lacy, DeVito, De Nivo, 2013). This results in the death of thousands of organisms, including *Spartina alterniflora* and *Spartina patens*, owing to a complete loss of oxygen (Cochran et al., 2018). The submergence of marshes repulses many waterfowl and birds that nest within them, and impedes healthy levels of environmental biodiversity (Swanson, O'Connell, Wilson, 2013). Both inundation and submergence result from anthropogenic climate change that is causing sea level to increase, a process that began with the exponential growth in human development during the 19th and 20th centuries, following the Industrial Revolution (Church et al., 2016; Moore, Holdsworth, Alverson, 2002).

Human development, recreation, and commercial activity along *Spartina* shores have resulted in stronger and more frequent wave action than naturally present (Gedan et al., 2008). Boats and jet skis speed through the mudflat channels within the marshes, causing catastrophic waves, both in force and number, which deteriorate salt marshes (Gedan et al., 2008). Human-induced wave action rips apart not only the root structures of marshes, but also pushes the mudflats farther back, resulting in marsh piling, whereby sediment is pushed upwards as the lower portions of marsh dissolve, leaving small cliffs and caves of marsh that eventually collapse from the weight of the piling (Lacy, DeVito, De Nivo, 2013; Moody, 2012).

Geukensia demissa, or ribbed mussels, along with other bivalves, play a role in marsh growth via filter-feeding. Ribbed mussels are unique in that there is little to no commercial market for them, and therefore they are not in danger of excessive harvesting. This is due to the fact that they are significantly harder to process for culinary purposes, and have an extremely unpalatable taste. Beyond that, ribbed mussels are more efficient at filter-feeding, with 60 percent more sediment deposition as compared to oysters (Moody, 2012).

Coastal marshes foster a synergistic symbiotic relationship between ribbed mussels and *Spartina* (Moody, 2012). Mussels provide nutrient-rich sediment via feces and pseudo-feces excretion that promote grass growth, while they simultaneously remove nitrogen from surrounding waters (Bilkovic, 2017) and add layers of sediment to the marsh in a process known as accretion (Moody, 2012). In return, the grasses act as a shelter from predators by allowing a location for the mussels to tether to with their byssal threads and raise spats, or young mussels. Called "living shorelines," marshes may be the key to preserving the wetlands long-term and preventing the damage caused by storm surge in future hurricanes that result from anthropogenic climate change (Davis et al., 2015).

It was hypothesized that ribbed mussel cover, *Spartina* grass presence, and environmental energetics influence the structure of marshes based on the different levels of interaction among these groups. Additionally, it was hypothesized that a "healthy" marsh environment contains flourishing levels of

Spartina and ribbed mussels, and environmental energy does not exceed that produced by ambient wave action.

Methodology

Measuring Environmental Energy

Mass transfer rates are an inexpensive and pragmatic way to generalize water energy and movement within a laboratory and field setting. The protocol was adapted from (Moody, 2012) and (Porter et al., 2000) to measure water flow rates within coastal marshes of Long Island, New York. Plaster-of-Paris hemispheres can be used to measure environmental energy (Moody, 2012; Yokoyama, 2004). The hemispheres measure mass-transfer rates, or the rate of dissolution of solute within a marine environment. (Yokoyama, 2004) gauged current energy in deep-water environments with such hemispheres, and (Moody, 2012) used hemispheres in a coastal marsh study to quantify wave action.

This study used mass-transfer meters, which were sanded by hand to 71 grams (± 1.5g), to measure the environmental energy, or wave energy, of the waters surrounding 10 disparate study sites in the coastal marshes of Freeport, New York.

Hemisphere Production

This study replicated the production of hemispheres as described in (Yokoyama, 2004) and (Moody, 2012), wherein the hemispheres were created by mixing plaster-of-Paris dry mix with water in a 2:1 ratio in a silicone mold originally purposed for cooking. The mix was then poured into 10 silicone trays, with each tray containing 6 individual hemisphere molds, for a total of 60 hemispheres. 50 hemispheres were put into use (5 per site across 10 sites), while 10 remained as backups if one of the field hemispheres broke before use. After molds were poured, a steel screw was inserted head-first into the center of each mold **(Fig. 1**). Each hemisphere was removed from the mold and allowed to dry for 72 hours, and then sanded to within 1.5 grams of one another as per (Moody, 2012), and dated to quantify time dried **(Fig. 1)**. The hemispheres were then screwed into a 1.27-centimeter-wide wooden dowel, which was prepared by drilling a hole into one end.

Hemisphere Deployment

Each hemisphere deployment corresponded to a transect, with 31 transects at each site. To measure mass transfer rates within the marsh area, each hemisphere deployment occurred within 5cm of the marsh edge, the location where mussels experiencing water flow would or would not be present (Moody, 2012). Hemispheres were spaced 37.5 meters apart (± 0.025m) across each 150-meter-long study site. One-meter-long wooden dowels were placed alongside the hemispheres to mark their locations. After 48 hours of deployment at the sites, each hemisphere was retrieved, rinsed in fresh water to remove salt, and allowed to dry for 48 hours inside aluminum foil pans, after which their final weights were measured on a scale.

Deployment had to occur during slack (intermediate) tide leading into low tide only, as the wetlands would have been submerged during slack tide leading into high tide, making safe deployment impossible.

Measuring Ribbed Mussel Cover

This study replicated the creation of a quadrat to measure mussel cover as described in (Moody, 2012). A single quadrat, measuring 25 centimeters by 25 centimeters (625 centimeters squared), was constructed with 2.54-centimeter-thick PVC piping and four PVC elbows. Sixteen perpendicular straight-line etchings were filed into the quadrat's frame to create grooves, with four etchings per side, spaced every 5 centimeters. Neon-yellow string trimmer cord was then stretched across each of the etchings, with 8 strings in all, to form a grid with 25 distinct squares. Finally, the entirety of the PVC piping was wrapped in three layers of black electrical tape to ensure the stability of the strings during fieldwork **(Fig. 2).**

In the field, the quadrat was placed every 5 meters (± 0.025) at each study site. Utilizing 8-mills-grade neoprene, 30.5-centimeter-long rubber gloves, mussel density was measured by placing the quadrat over the wetland surface, whether it was a mudflat covered in marsh grass or an eroded sandy beach, and mussels were counted one square at a time, for a total of 7,750 discrete data points across the 10 sites **(Fig. 2, Fig. 3)**.

Data for each square was recorded in a waterproof notebook provided by Hofstra University with a black Sharpie marker, and each quadrat was then photographed. This process was repeated 31 times per 150-meter study site, for a total of 310 quadrat measurements **(Fig. 3).**

Measuring Spartina Cover

Spartina cover was measured for each site using photographic analysis. Photographs of each of the 31 quadrats used within each site were taken, and depicted *Spartina* presence and cover. An average percent cover of each site (n=10) was determined by averaging the percentage of *Spartina* present within each quadrat measurement (n=31).

Location/Site Selection

Potential study sites were initially mapped out using the National Wetlands Inventory, an online public-domain database published and maintained by the U.S. Fish and Wildlife Service. A diversity of study sites was selected to mimic (Moody, 2012) and (Porter et al., 2000). Field research locations were determined according to two central criteria: location accessibility and terrain variability in accordance with categorizations introduced by (Moore, 2002). Such categorizations included: "flourishing", "intermediate", and "dead" marshes. In addition, distance to heavily trafficked boat channels was considered during site selection. A mix of close and distant sites was chosen **(Fig. 4)**.

Examples of each site were confirmed locally during 12 scouting trips over the course of 50 hours in May and June of 2019. Such trips reached as far as eight kilometers. Kayaks were launched from four sites during this process: the Norman J. Levy Park and Preserve in Merrick, New York, where Merrick Bay and its surrounding wetland channels were explored; Cow Meadow Park and the Albany Avenue boat launch

in Freeport, where the Narrows were scouted; and Waterfront Park in Freeport, where Middle Bay, between Freeport and Baldwin, was explored **(Fig. 4)**.

Reaching Study Sites

Kayaks were used to reach each study site, as they provided a carbon-free means of transportation, as opposed to a carbon-intensive motorboat that would have further contributed to the ongoing climate crisis. Moreover, a motorboat would have damaged the wetlands when landing and departing from mudflats. Kayaks were transported by car to one of three launches: the southern end of Albany Avenue in the Village of Freeport; the southern end of Woodcleft Avenue in Freeport at the Waterfront Park kayak launch site in Freeport. Kayaks were then carried to the shoreline, and all equipment was stowed inside the kayaks.

Material Allocation, Management, and Safety

The plaster-of-Paris, dowels, and screws were purchased from the Freeport Home Depot, and the silicone cooking molds were ordered from a wholesale cooking-supply company via Hofstra University. The scale used for measuring hemispheres was provided by Hofstra University. Proper Personal Protective Equipment (PPE) and Safety Data Sheets (SDS) were studied before working with plaster-of-Paris, a known carcinogen in a particulate state. Goggles, gloves, a full-body suit, and respirator were worn during sanding, which took place outdoors under the supervision of Hofstra University Professor Dr. Emma Farmer. Additionally, the author contacted the Uniondale Fire Department to have the work area approved.

Kayaks were purchased from outdoor outfitter Recreational Equipment, Inc. (REI), in Carle Place, New York. Leg-length waders were purchased from Dick's Sporting Goods, a sporting/activity wholesale store in Garden City, New York. Lifejackets were worn at all times, including at study sites, and a first-aid kit was stored in a waterproof safety bag during each field trip. And this author was accompanied at all times by his father in the field, for safety's sake.

Kayaks were washed down twice after each trip — once at the site with five 3.8-liter water containers to remove larger debris and mud, and a second time at home with a garden hose. All equipment was also washed down each time to remove salt and debris and left outside to dry overnight. All equipment, including hemispheres for deployment, was stored in the author's home garage.

Results

It was hypothesized that ribbed mussel cover, *Spartina* grass presence, and environmental energetics influence the structure of marshes based on the different levels of interaction among these groups. Environmental energetics were measured using mass-transfer meters made of plaster-of-Paris, which mimicked marsh erosion rates in the form of mass-transfer rates, in grams-per-hour (*MT Rate*). Mussel coverage and Spartina coverage data were collected via transect assays 150 meters in length across 10 disparate sites in Freeport, New York, and quantified via percentages.

It was found that “healthy” marshes contain “flourishing,” or high, levels of both ribbed mussels and *Spartina*. An absence or near-absence of “flourishing” amounts of either mussels or *Spartina* resulted in the development “intermediate” or “dead” marshes, suggesting that marsh health relies heavily on the relationship between mussel presence and *Spartina* grasses. It was also observed that mussels not tethered to *Spartina* are more likely to be washed away by even ambient wave action, as verified by 17 minutes of videography depicting marsh decay in real-time. Also, the mussels present in flourishing areas were observed to be larger in length, an indication of age corroborated in (Moore, 2002) and (Moody, 2012).

Additionally, when mussels and *Spartina* are “flourishing” together, mussels prefer lower-energy environments **(Fig. 9B)**, and data suggest this may promote accretion, represented by a negative mass-transfer rate. If a low energy environment encourages mussel growth and maturity as described in (Moody, 2012), then a negative mass-transfer rate could indicate possible accretion. The negative mass-transfer rate for site 3 was determined by calculating a gain in mass after identical periods of drying time and environmental exposure as the other nine sites; however, when mussels and *Spartina* are not concurrently present, a “dead” or “intermediate” marsh forms, identified within the study by observing little to no mussel or *Spartina* growth.

Historical Comparison

Historical data were obtained in the form of maps. 2-dimensional maps were used to compare coastal marshes in Freeport, New York, in 2019 to that of marshes dating to 1903, a 116-year difference **(Fig. 5)**. Data were also collected from 1892 to assess land organization within the South Shores of Long Island, New York (data not shown). In 1903, land archives were recorded as school district zones, and the oldest reliable record of coastal marshes in Freeport, New York, dates to 1903. Maps from 1892 assisted in understanding human development on Long Island; however, the 1903 map included the first named parcels of marsh, a signifier of nearby human development. Trends in human development and consequential impact were established by visually comparing the 1903 map to a map of the same location dated in October of 2019, which was obtained from Google Maps, a publicly accessible website that gives a 2- and 3-dimensional view of the entire Earth. 2-dimensional maps were used for consistency with the 1903 map and to establish linear accuracy.

From visual comparisons, it was discerned that over the past 116 years, human development in Freeport, New York, has changed marshes dramatically. Coastal marsh area depicted in the 1903 map **(A)** is 2,809 to 3,481 square meters ($56m^2 \pm 3m^2$) larger than coastal marsh area from the 2019 map **(B)**. This area is equivalent to 1.4 to 1.7 times that of the Vatican, a representation of the amount of marsh that has been destroyed since 1903. Additionally, it can be observed that dramatic changes to inland development influence marsh stability. In 1903, the Meadowbrook Parkway, the 20-kilometer stretch of road that runs southwards within the right-hand side of **(B)**, did not exist. Its creation was made possible between 1932 and 1962 by the clearing of marshes, a trend that was observed within proximity to the parkway.

Environmental Energetics of Location 1: Freeport Creek
Environmental Energetics of Location 2: Smith Meadow

This study investigated environmental energetics. Wave energy was analyzed within the context of coastline erosion, similarly described in (Moody, 2012). Mass-transfer rates were used to quantify such energies **(Table 1, Table 2, Table 3, Table 4).** Mass-transfer rates were measured at 5 points within each site (n = 10), with each point 37.5 meters away from one another beginning at the starting point of the transect. The meters were left out for 48 hours, and their masses after this period were collected and compared to that of their starting masses, producing a subsequent loss in grams, percentage loss, and loss-per-48-hours **(Table 1, Table 2, Table 3, Table 4).**

It was found that distance heavily influences environmental energy within a marsh environment. For example, the data from sub-location of Freeport Creek Island **(Fig. 6, Table 1)** show how transects **(B)** and **(C)** are extremely similar in distance relative to the northern-most tip of the island (where **(B)** and **(C)** converge). **(C)** was found to be insignificantly farther south when compared to **(B)** ($p > 0.05$). This indicated that the relative distance difference between **(B)** and **(C)** did not impact the mass-transfer rates measured. The distance of **(A)** relative to the northern-most tip of the island was significantly greater than that of **(B)** or **(C)** ($p < 0.04$). Additionally, the mass-transfer rates of **(A)** were found to be dramatically larger than those of **(B)** or **(C)**, with **(A)** having double the mass-transfer rate of **(B)** or **(C).**

In the Smith Meadow sub-location, a similar trend was observed, with the northern-most side of the meadow having ~ 60% the mass-transfer rate of the eastern side **(Table 2)**. A near-identical finding was observed at the Freeport Creek Rocky Beach sub-location, with the northern-most measured transect **(A)** having ~ 65% that of the southern-most assessed region **(B) (Fig. 7, Table 2).** Additionally, a near-identical percent difference was observed for the mass-transfer rates between the Freeport Creek Rocky Beach and Freeport Creek Island, with the northern-most assay of Freeport Creek Rocky Beach being ~ 63% that of the southern-most assay of Freeport Creek Island.

Smith Meadow Island produced both a positive and negative mass-transfer rates between sites. These data indicate that the island's "front", or eastern-most side, is more susceptible to marsh erosion than the "back", or western-most side, as the mass-transfer rate of the eastern-most site is significantly greater than that of the western-most side. The mass-transfer rate of the western-most side produced a negative mass-transfer rate, which indicated that mass was *added* to the mass-transfer meters **(Table 4 (B)).** This finding demonstrates that environmental energy was low enough to allow for the rate of accretion, or wetland mass gain, to outpace that of dissolution, or erosion, of the mass-transfer meters. As such, it was found that the use of boat channels heavily influences environmental energy, and in the absence of such disturbance, as is the case in the eastern-most side of Smith Meadow Island, accretion outpaces the rate of erosion.

This finding confirms the idea that anthropogenic (human-caused) energy increases as southward distance increases. In fact, the points of significance within each site-location appear to depend on the levels of energy found in the wake-zones, which are loosely enforced, if at all. The point where the

transects converge at Freeport Creek Rocky Beach **(Fig. 7)** is the very same point where the no-wake zone ends for Freeport Creek as a whole. Additionally, the western-most site within the Smith Meadow Island sub-location is devoid of boats or jet skis for a minimum distance of 57 meters westward and a maximum distance of 183 meters northward, leaving a large area inaccessible to humans **(Fig. 9)**. This supports the idea that where human impact is *absent*, levels of marsh erosion are limited only to that produced by ambience, or the natural environmental energy, and may promote accretion, indicated by the negative mass-transfer rate of Smith Meadow Island's western-most site.

Mussel Coverage

Ribbed mussel coverage was measured using quadrat data acquisition across each site's 150-meter-long transect. Procedures were adapted from (Moody, 2012). Field probing of 310 quadrats was performed to assay mussel coverage, and photographs were taken of each quadrat, later used as a secondary source of mussel presence confirmation **(Table 5)**. The averages of each site's mussel coverage were then calculated, graphically represented in **(Fig. 10)**.

These data indicate that mussel coverage and marsh health are linked. 9 out of 10 sites had less than 30% mussel coverage, with the remaining site less than 40% **(Fig. 10, Table 5)**. All accessible sites had immense regions of dead marsh, and flourishing marshes were an average of 4.4 meters inland from the shoreline. Additionally, it was found that Site 2, a site within the Smith Meadow sub-location **(Fig. 8 (B))**, had the largest percent coverage, with an average of 37.94%. While this numerical significance was established, the applicability of such a number is inflated based on the geology of the correspondingly assayed land. This number was shown to be significantly higher than the 9 sites across the study, but this significance does not justify a suggested interpretation of a healthier marsh. Through observation and photographic evidence, it was determined that the significance of this number can be attributed to the fact that the marshes in its respective site were frequently undercut and outcropped, leaving only a small intermediate sector of marsh, which ultimately made the distance from the shore to measurable land shorter, proportionately inflating the recorded percent coverage.

Mussel Coverage Assessment

Spartina Coverage

Spartina coverage was measured using quadrat data acquisition across each site's 150-meter-long transect, with procedures adapted from (Moody, 2012). Field probing of 310 quadrats was performed to assay mussel coverage, and photographs were taken of each quadrat, later used as a secondary source of mussel presence confirmation **(Table 6)**. The averages of each site's *Spartina* coverage were then calculated, graphically represented in **(Fig. 11)**.

Ribbed mussel and *Spartina* data collected showed a positive link between mussel coverage and *Spartina* coverage. Essentially, where mussels were present, *Spartina* was also present, and in areas where mussels were absent, *Spartina* were proportionately absent. *Spartina* data also support one of the pre-

field-work predictions, which stated that mussels have a higher degree of dependence on *Spartina* than *Spartina* have on mussels. This assertion is supported by the fact that the investigated sets of mussels show a larger range of difference in percent coverage when compared to a hypothetical *Spartina* coverage constant, and *Spartina* have a 20% smaller range for percent coverage when compared to a hypothetical ribbed mussel coverage constant. These data, however, while able to demonstrate a trend, do not quantify a specific rate of mussel-to-*Spartina* dependence; rather, they confirm the validity of an observed symbiotic relationship between *Spartina* and mussels.

Decay-Rate Model of Salt Marshes

As previously stated, marshes on Long Island were found to have a decay-rate 6.5 to 20 times that of the most recently measured national rate. This study employed a novel set of logic-based algorithms that consider marsh decay-rates as a symptom of erosion. The model follows the assumption that mass-transfer rates were established beforehand, as was done in this study. The model is as follows:

1. Adjust mass-transfer rates based on the density of any given marsh (14% increase within this study) for any given length of marsh occupying the shoreline.
2. To create a degree of accuracy, shorelines must be measured in 1-square-meter intervals, wherein the inland-reach of such an interval does not exceed 1 meter. The linear distance can then be quantified in meters while maintaining dimensional accuracy.
3. Convert square meters to acre feet to find a measurable volume from any given area. Conversions from square meters to acre feet can correctly be made; thus, converting marsh area loss is able to be quantified in all three dimensions.
4. Quantify over a time period (in this study, years were used) to determine total marsh loss. This step of analysis can then be reversed to obtain the quantity of time left for any given area of marsh, a process that was used in this study.

Discussion

This study predicts a near-total loss of Long Island's wetlands by the year 2079. It is estimated that submergence, a result of sea-level rise (Brandon et al., 2014; Lacy, DeVito, De Nivo, 2013), alone could lead to a 20 percent loss of wetland cover throughout the U.S. by the end of the 21st century (Moody, 2012). The State of Delaware, as described in (Kreeger et al., 2017), reached that conclusion, predicting its coastal wetland losses in excess of 90 percent by the turn of the century. This study demonstrates that the disparities between marsh predictions exist on a range, and that national predictions may not be accurate locally, as they do not account for the numerous factors that have an outside influence on marsh decay within specific regions and sites.

In a healthy shoreline marsh ecosystem, wetland erosion decreases as ribbed mussel density increases (Moody, 2012). The mussels aid in shoreline stabilization, acting as “hard armoring” against wave action and tidal surge. The mussel aids in vertical wetland accretion by the deposition of feces and pseudo-feces (Moody, 2012), becoming, in effect, the salt marshes’ first and strongest defense against rising anthropogenic sea level rise, an affliction currently observed on Long Island, New York.

This study found that ribbed mussel coverage throughout the 10 sites that were examined with transect measurements was scarce to non-existent. Of the 10 sites, only one site – Site 2 – had mussel coverage that reached above one-third, at 37.94 percent. Three sites were in the 10 to 12 percent range. The remaining six sites had mussel coverage from zero to 6.7 percent. These sites were categorized as dead or near-dead marsh, categorizations described in (Moore, 2002), with only rocky beach and remnants of peat (partially decomposed plant matter) remaining. In a stable wetland ecosystem, it is expected that ribbed mussel cover would be at or near 100 percent at the marsh edge, with mussel populations as high as 2,000–3,000 per square meter according to (Moody, 2012). Thus, the marshes in Freeport, New York, are not healthy; in fact, they are steeply below the healthy categorizations of (Moore, 2002) and (Moody, 2012). 9 out of the 10 study sites – and much of the surrounding marshes, which were later observed – can be categorized as dead marsh.

Site 5 saw the second-highest level of anthropogenic wave action, with a mass-transfer rate of 0.57 grams per hour, or a 34.57 percent net mass loss. Site 5 was located on the demarcating line of a no-wake zone, where boaters tend to open up their engines and speed due south, causing a steady stream of strong waves to cascade against the shoreline. Site 7 recorded the third highest wave action, at 0.53 grams per hour, or a 25.44 percent net mass loss. Site 7 was located directly across from Site 5 to the west. The calculated ratios between such energetics, as mentioned in “RESULTS”, indicate that as assays gained southward distance from each respective site’s starting point, energy levels increased. (Yokoyama, 2006) demonstrates that as environmental energy increases, erosion rates and water flow increase proportionately.

Thus, within the marshes of Freeport, New York, southward distance gain results in higher levels of environmental energy and subsequent levels of erosion. This is significant because in Freeport, New York, boat channels move southwards, meaning that the trends found within this study are verified based on the directional trend of environmental energetics described by (Yokoyama, 2006). These findings also confirm the idea that increased energetics result in increased levels of erosion, and strongly suggest that heavily trafficked boat channels dramatically increase coastal marsh erosion, causing *Spartina* to die and mussel beds to be swept away bit by bit.

In the absence of coastal marshes, sand is allowed to wash farther inland, coating entire sections of marsh such that *Spartina*, mussels, and all other life forms suffocate and die. This, in turn, compromises the structural integrity of the marshes, making it vulnerable to erosion and eventual disintegration. Peat beds devoid of mussels and *Spartina* become weakened, and meter-long chunks of marsh fall into the water, as was frequently observed in the field. Undercutting, another form of erosion that exposes the

roots of *Spartina*, and results from abnormal, human-induced wave action, was observed. This type of erosion, which was widely observed in this study, exposes the root structures of *Spartina* from below, causing them to perish. Such destruction is a potentially catastrophic threat to the thousands of communities on the Atlantic Coast, like Freeport, but is preventable.

This study had minor limitations that caused certain data to form ranges, rather than set values. First, it is impossible to procedurally predict an event that the future holds, particularly with environments vulnerable to dramatic changes, as salt marshes are. The results of anthropogenic climate change can result in an immeasurable number of possible changes to the environment, and thus a calculated range had to be produced for observed wetland loss and total wetland loss prediction. Additionally, mass-transfer rates had a level of variance within each site that slightly influenced the differences in mass-transfer rates between sites, but not the outcome of trends observed.

Once the process of erosion has begun, it becomes clear that it is impossible to stop without human intervention. With every chunk of peat bed that dissolves into surrounding waters, the structural integrity of the marsh is weakened until all that remains are lifeless tracts of clay and sand, unable to support life, in particular ribbed mussels, which depend on a steady supply of seawater for survival. A number of lifeless clusters of mussels were observed on chunks of broken peat that had washed up on a sandy beach, dying as they baked in the summer sun, a reminder of future marshes if none of the much-needed intervention occurs. Only by correctly identifying regions afflicted by coastal marsh decay, and addressing the symptoms of climate changes with widely applicable public policy, can we hope to reshape the future for the betterment of humanity.

Conclusion

This study was the first to examine wave energetics and ribbed mussels within the salt marshes of Long Island, New York. Additionally, *Spartina*, ribbed mussels, and wave energetics have never before been studied with the purpose of promoting marsh restoration on Long Island. It was determined that the annual rate at which wetland mudflats are disintegrating is 0.66 percent-marsh-cover per year. Seemingly insignificant, this number is 6.5 to 20 times that of the most current national rate, and suggests that national estimations may be inaccurate by a large factor – both in years and in marsh area. Given such dire conditions, without aggressive intervention to preserve salt marshes, it was estimated – through a novel decay-rate model – that Long Island could lose all of its wetlands by the year 2079. This demonstrates the need for immediate action, and for the introduction of public environmental policy to maintain Long Island's salt marshes. Such policy could be shaped around areas that quantify the need for marsh preservation, as was done in this study, and would help ensure the safety of an estimated 3 million people native to Long Island in the event of a catastrophic hurricane – an inevitable affliction for future Long Islanders according to (Brandon et al., 2014).

Wetland loss is accelerating nationwide (Stedman *e. a.l*, 2008) owing to an array of factors. According to (Moody, 2012), wakes caused by motorboats and jet skis can cause heavy wave action, an idea

confirmed by this study. Nitrogen-loaded fertilizer runoff can also heavily impact the biology of marshes, resulting in chemical marsh disintegration that can cause peat to collapse, thus destroying marshes (South Shore Estuary Reserve Council, 2016; Wallace, et al., 2014). Submergence resulting from rising oceans is a threat already afflicting coastal marshes by drowning out many of their core species such as *Spartina* and ribbed mussels, and tear apart the coast (Flavell *et a.l*, 2019).

This study combined field observation, numerical, and historical data to form a body of evidence that strongly suggests ribbed mussels (*Geukensia demissa*) play an integral role in the maintenance of salt marsh mudflats. These bivalves exist in a synergistic symbiotic relationship with *Spartina*, and strongly enhance the ability of *Spartina* to hold together the mudflats by promoting the growth of their expansive root systems, which descend deep into the peat beds. This study, which confirmed such a relationship, supports the idea that when either of these core species is absent, marshes disintegrate.

Mussels benefit marsh health by filtering dissolved solids from surrounding waters and depositing them onto the wetlands, increasing marsh size. To promote this process – known as accretion – local governments, such as the Town of Hempstead on Long Island, should begin a campaign to seed coastal marshes with ribbed mussels. At the same time, local governments must better enforce no-wake zones to ensure that heavy wave action caused by boats and jet skis does not continue to erode the mudflats. This study found that mussel and *Spartina* coverage was thicker in less trafficked boat channels and thinner in more heavily traveled channels.

Artificial storm-surge barriers, such as the floodgates found in New Bedford, Connecticut, have been proposed for the Village of Freeport, New York (Nataly, 2018), where this study was conducted. The village, a mix of suburban housing, heavy industry, and marinas, suffered among Long Island's greatest losses of homes and businesses during Superstorm Sandy, and is still under repair on various streets closest to wetland channels seven years later. The Freeport administration proposed the tidal gates in 2016 as a means to protect the South Shore in the event of a hurricane. The municipality, however, does not have the economic means to independently construct the gates, and therefore is dependent on the federal government to complete the project. The price of construction is estimated at $300 million (Nataly, 2019).

Seeding of the wetlands with ribbed mussels to accelerate mudflat accretion, coupled with aggressive enforcement of boating laws to prevent further wetland degradation, would present an immediate, relatively low-cost solution to enhancing Long Island's shoreline defenses against oceanic storms. Further studies are needed to determine whether the levels of wetland dissolution observed on Long Island are found in other similar suburban/urban environments across the U.S. Public policy should target such communities for wetland restoration projects using natural means like ribbed mussel seeding. The Earth is reaching its tipping point (500ppm of atmospheric CO_2), after which climate change will become uncontrollable (Jones, 2017). Immediate action is required.

Declarations

Acknowledgements

I would like to thank my research mentor, Dr. Emma Farmer, Hofstra University Professor; Mr. Kyle Rabin, program manager of Long Island Nitrogen Action Plan; Mr. Richard Guardino, executive director of the Long Island Regional Planning Council; Mr. Morris Kramer, Long Beach barrier island citizen scientist and environmentalist; and Dr. Jim Brown, Town of Hempstead biologist, for their guidance and encouragement.

I would also like to thank Mrs. Barbi Frank, John F. Kennedy High School Advanced Science Research teacher, for her commitment to excellence in research and her continuous support. Most importantly, I would like to thank my family — my parents, sister and grandmother — for their never-ending love and encouragement throughout my research endeavors.

Funding:

The author (AB) funded this study in its entirety.

Conflict of Interest:

Not applicable.

Ethics Approval:

Ethics were discussed with the Town of Hempstead to ensure the study was non-invasive. All probes left in the field replicate the materials found within the natural environment and are not harmful to the ecosystem or any/all living things. The study was conducted entirely within the public realm. No private property was traversed or studied.

Consent to Participate:

Not applicable.

Consent for Publication:

Not applicable.

Availability of Data and Material:

All data was collected from the public domain or was generated by the AB. The datasets used and/or analyzed during the current study are available from the corresponding author on reasonable request. All data produced from this study are provided in this manuscript.

Code Availability:

AB author used Microsoft PowerPoint, Excel, and Word.

Author's Contributions:

The author of this study (AB) is the sole producer of this manuscript, and was generated entirely from the author (AB).

Endnotes

1. Andrew Brinton; photos taken on personal camera; 2019
2. Includes procedures replicated from (Moody, 2012).
3. Map data was acquired through Google Earth, a website available to the public; historical maps used were from the Town of Hempstead Archives, a historical data collection available to the public. Used with permission from both sources.

References

1. Bilkovic, D. M., Mitchell M. M., Isdell, R. E., Schliep, M., Smyth, A. R., 2017. "Mutualism between ribbed mussels and cordgrass enhances salt marsh nitrogen removal". *Ecosphere* 8(4):e01795. doi: 10.1002/ecs2.1795
2. Bowman, J., 1990. "The greenhouse effect". *Land Use Policy* Volume 7, Issue 2, April 1990, Pages 101-108 doi: 10.1016/0264-8377(90)90002-G
3. Brandon, C.M., et al., 2014. "How Unique was Hurricane Sandy? Sedimentary Reconstructions of Extreme Flooding from New York Harbor" *Scientific Reports* 2014/12/08/online, Volume 4;7366 10.1038/srep07366
4. Chaisson, B., 2018. "What We Know (and Don't Know) About Sea Level Rise". *Center for Climate and Life, Lamont-Doherty Earth Observatory, Columbia University Earth Institute*
5. Church, J.A., et al., 2016. "Anthropogenic forcing dominates global mean sea-level rise since 1970". *Nature Climate Change* Volume 6, pages 701–705 (2016) doi: 10.1038/nclimate2991
6. Cochran, J. K., et al., 2018. "Health and Resilience of Salt Marshes in Jamaica Bay, NY". *Natural Resource Report, Geochemical and Dynamical Perspectives* NPS/NCBN/NRR––1643

7. Colle, B.A., et al., 2008. “New York City’s Vulnerability to Coastal Flooding”. *American Meteorological Society* doi: 10.1175/2007BAMS2401.1
8. Dahl, T.A., 1990. “Wetlands Loss Since the Revolution”. *National Wetlands Inventory Newsletter,* Volume 12, No. 6, Environmental Law Institute, Washington, D.C.
9. Davis, J. L., et al., 2015. “Living Shorelines: Coastal Resilience with a Blue Carbon Benefit”. *PLoS One* 10(11):e0142595 doi: 10.1371/journal.pone.0142595
10. Environmental Protection Agency, Report on the Environment, undated Internet publication from EPA.gov. “Greenhouse Gases: What are the trends in greenhouse gas emissions and concentrations and their impacts on human health and the environment?”
11. Flavell, C. and Lu, D., 2019. “Rising Seas Will Erase More Cities by 2050, New Research Shows”. *The New York Times*
12. Gedan, K.B, Bertness, M. D., 2010. “How will warming affect the salt marsh foundation species *Spartina patens* and its ecological role?”. *Oecologia, Community Ecology* (2010) doi: 10.1007/s00442-010-1661-x
13. Gedan, K. B., et al., 2008. “Centuries of Human-Driven Change in Salt Marsh Ecosystems”. *Annual Review of Marine Science* doi: 10.1146/annurev.marine.010908.163930
14. Jain, P.C., 2003. “Greenhouse effect and climate change: scientific basis and overview”. *Renewable energy* doi: 10.1016/0960-1481(93)90108-S
15. Jones, N., 2017. “Breaking Records: How the World Passed a Carbon Threshold and Why It Matters”. *Yale360, published by the Yale School of Forestry & Environmental Studies*
16. Kreeger, D., Moody, J., Padeletti, A., Whalen, L., December 2017. “Constructing Bio-based Living Shorelines to Stem Erosion of Salt Marshes in New Jersey: Final Report for the New Jersey Department of Environmental Protection”. *Partnership for the Delaware Estuary — A National Estuary Program*
17. Kroeze, C., 1992. “Nitrous oxide and global warming”. *Science of The Total Environment*
18. *Volume 143,* Issues 2–3, 15 April 1994, Pages 193-209 doi:10.1016/0048-9697(94)90457-X
19. Lacy, H.S., DeVito, A., De Nivo, A. C., 2013. “Geotechnical Aspects of Three Storm Surge Barrier Sites to Protect New York City from Flooding”. *Storm Surge Barriers to Protect New York City, ascelibrary.org by Columbia University*
20. Moody, J. A., 2012. “The relationship between the ribbed mussel (Geukensia demissa) and salt marsh shoreline erosion” *Masters thesis submitted to the Graduate School at Rutgers, the State University of New Jersey* doi:10.7282/T3TT4PW8
21. Moore, G.W.K., Holdsworth, G., Alverson, K., 2002. “Climate change in the North Pacific region over the past three centuries”. *Nature* (2002) Nov 28;420(6914):401-3. doi: 10.1038/nature01229
22. Nataly, N., 2018. “Freeport officials, hoping to construct floodgates here, tour Massachusetts project”. *Freeport Herald-Leader*

23. Nataly, N., 2019. "'Waiting for 2030 is unacceptable': Residents angry — study offers no flooding solutions". *Freeport Herald-Leader*
24. Porter, Elka T., Lawrence P. Sanford, and Steven E. Suttles. 2000. "Gypsum Dissolution Is Not Universal Integrator of 'Water Motion'". *Limnology and Oceanography.* 54(1): 145-158.
25. Solomon, S., Plattner, G. K., Knutti, R., & Friedlingstein, P., 2009. Irreversible climate change due to carbon dioxide emissions. *Proceedings of the National Academy of Sciences of the United States of America*, *106*(6), 1704–1709. doi:10.1073/pnas.0812721106
26. South Shore Estuary Reserve Council, 2016. "Long Island South Shore Estuary Reserve Eastern Bays Project: Nitrogen Loading, Sources, and Management Options" *Prepared for the New York State Office of Planning and Development*
27. Stedman, S. and Dahal, T.E., 2008. "Status and Trends of Wetlands in the Coastal Watersheds of the Eastern United States 1998 to 2004". *National Oceanic and Atmospheric Administration, National Marine Fisheries Service, and the U.S. Department of the Interior, Fish and Wildlife Service*
28. Swanson, R.L., O'Connell, C., Wilson, R.E., 2013. "Storm Surge Barriers: Ecological and Special Concerns". *Storm Surge Barriers to Protect New York City: Against the Deluge* ISBN (print): 9780784412527ISBN (PDF): 9780784477007 doi: 10.1061/9780784412527
29. "Threats to Wetlands: What is the Status of Our Nation's Wetlands?" September 2001. *U.S. Environmental Protection Agency*
30. Town of Hempstead School District Boundaries Map, 1903
31. Town of Hempstead Water Quality Report 1975-2012, *Department of Conservation and Waterways entry*
32. Wallace, R. B., Baumann, H., Grear, J. S., Aller, R. C., Gobler, C. J., 2014. "Coastal ocean acidification: The other eutrophication problem" *Estuary, Coastal and Shelf Science* Volume 148, 5 July 2014, Pages 1-13 doi: 10.1016/j.ecss.2014.05.027
33. "What Are Coastal Wetlands?" *Science and Climate Defined*, undated Internet publication from the University of California at Davis
34. Yokoyama, 2004. "Estimation of the assimilative capacity of fish-farm environments based on current velocity measured by plaster balls." *Aquaculture* 240; 233-247.

Figures

Figure 1

Mass-Transfer Meters. 50 individual mass-transfer meters were constructed to measure the dissolution of Plaster-of-Paris, a material with a similar density to that of soil1,2.

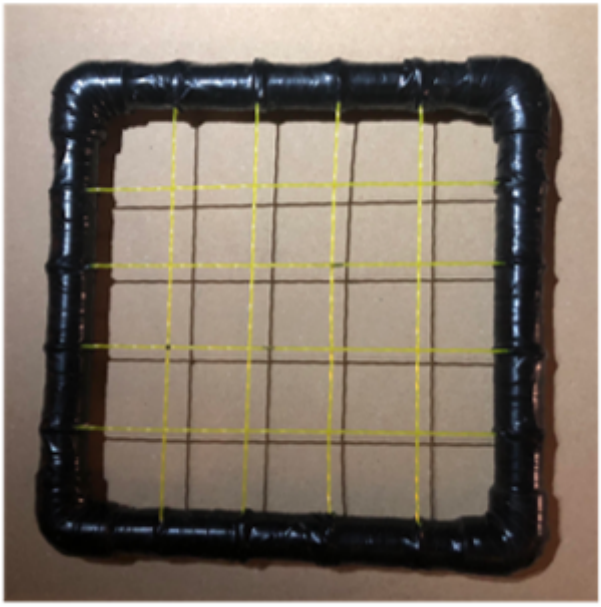

Figure 2

625cm2 Quadrat. A quadrat was constructed out of PVC piping and lawn trimmer wiring. Each box on the created grid corresponds to 4% coverage, becoming the bases for assaying mussel coverage as a percentage. Both photographic and physical probing were used to corroborate mussel presence within the grid1,2.

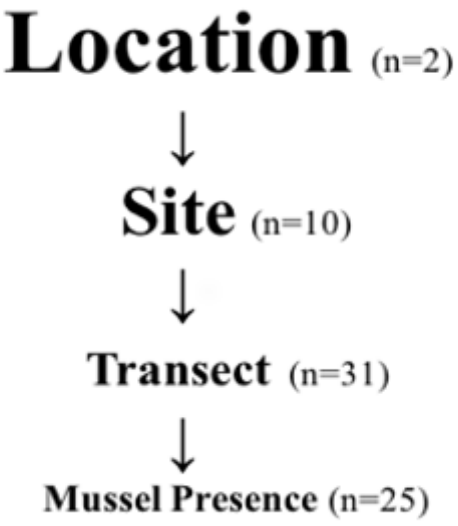

Figure 3

Schematic Design of Marsh Assays. 2 locations were selected for study. Within each site, 10 sites were determined for study. In each site, 31 transects were performed across a 150-meter-long span of marsh edge. In each transect measurement, mussel coverage was probed 25 times.

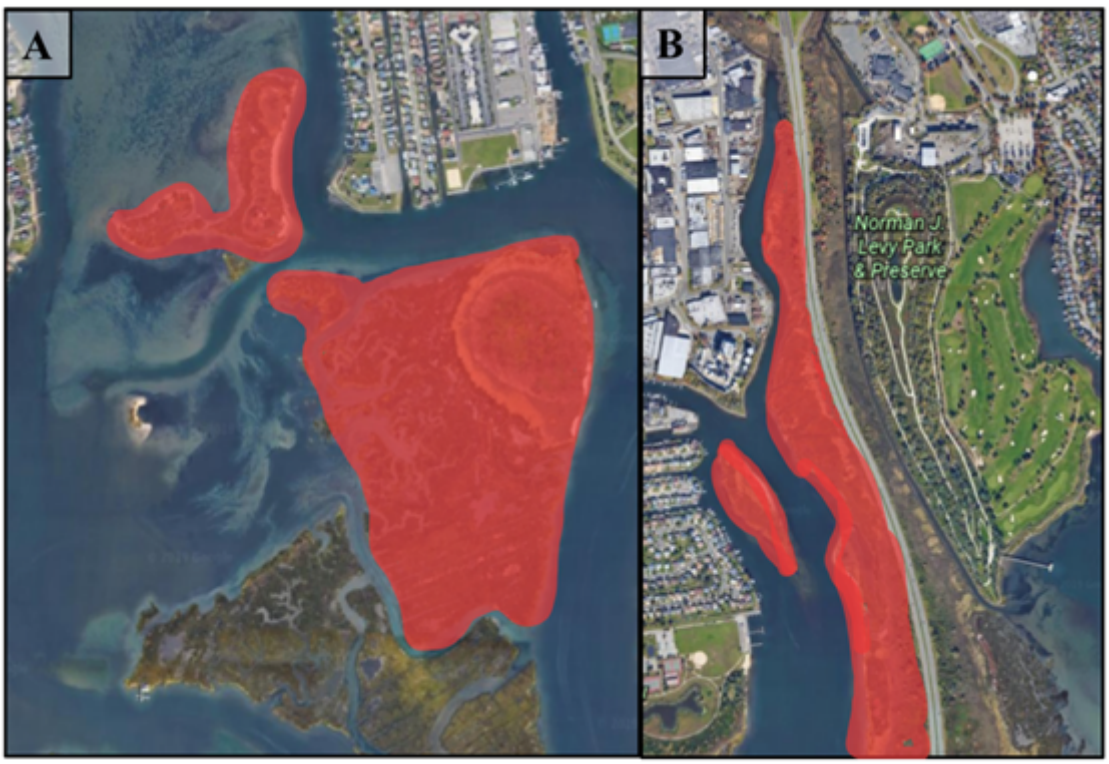

Figure 4

Location Selection. Locations Smith Meadow (A) and Freeport Creek (B) were chosen for investigation. The 10 study sites are located within the map portions highlighted in red.

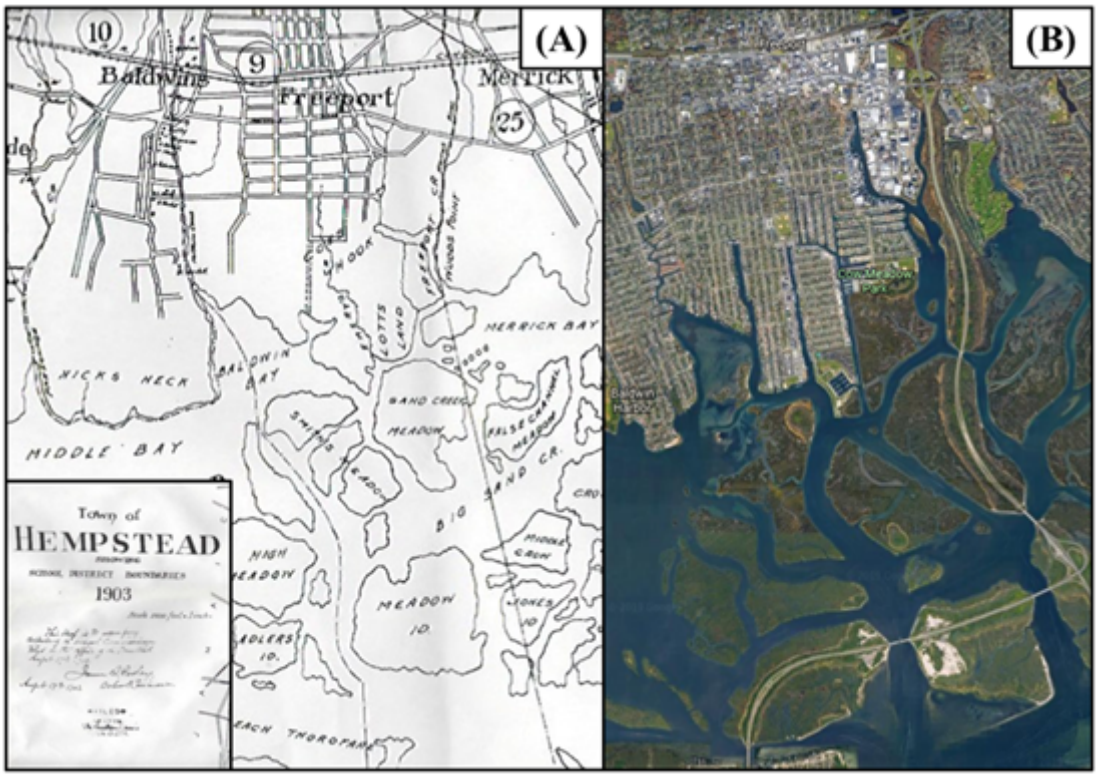

Figure 5

Historical Data Comparison. Historical figures were obtained via the Town of Hempstead Archives in New York, which is a data repository available to the public. The data shown are maps of Freeport from 1903 (A) and 2019 (B). The lower left-hand corner of map (A) depicts the Town of Hempstead Archives confirmation that the map was hand-drawn in 1903. Each map contains both Smith Meadow and Freeport Creek study locations. Map (A) has an accuracy of 3 meters, and map (B) has an accuracy of 1 meter.

Site 7	FREEPORT CREEK ISLAND SIDE 1			(A)
Location	Loss (g)	Loss (%)	MT Rate (g/hr)	
L1	30.28	27.40	0.63	
L2	23.12	23.11	0.48	
L3	12.84	18.08	0.27	
L4	24.53	25.73	0.51	
L5	35.30	32.88	0.74	
Average	25.21	25.44	0.53	
Site 4	FREEPORT CREEK ISLAND SIDE 2			(B)
Location	Loss (g)	Loss (%)	MT Rate (g/hr)	
L1	17.75	25.00	0.37	
L2	12.50	17.61	0.26	
L3	3.61	5.08	0.08	
L4	12.21	17.20	0.25	
L5	14.17	19.96	0.30	
Average	12.05	16.97	0.25	
Site 8	FREEPORT CREEK ISLAND SIDE 3			(C)
Location	Loss (g)	Loss (%)	MT Rate (g/hr)	
L1	11.59	10.49	0.24	
L2	-6.70	-9.44	-0.14	
L3	17.81	22.31	0.37	
L4	17.29	19.15	0.36	
L5	17.27	17.12	0.36	
Average	11.45	11.93	0.24	

Figure 6

Environmental Energetics of Location 1: Freeport Creek (Top) Figure 6: Freeport Creek Island. Freeport Creek Island comprised 3 out of the 5 total sties for the Freeport Creek study location. The highlighted sections (A), (B), and (C) correspond with the following identically labeled tables. (Bottom) Table 1: Mass-Transfer Rates of Freeport Creek Island. Mass-transfer rates were gathered at 5 evenly distanced points along each 150-meter-long transect, labeled as L1-L5 within each site.

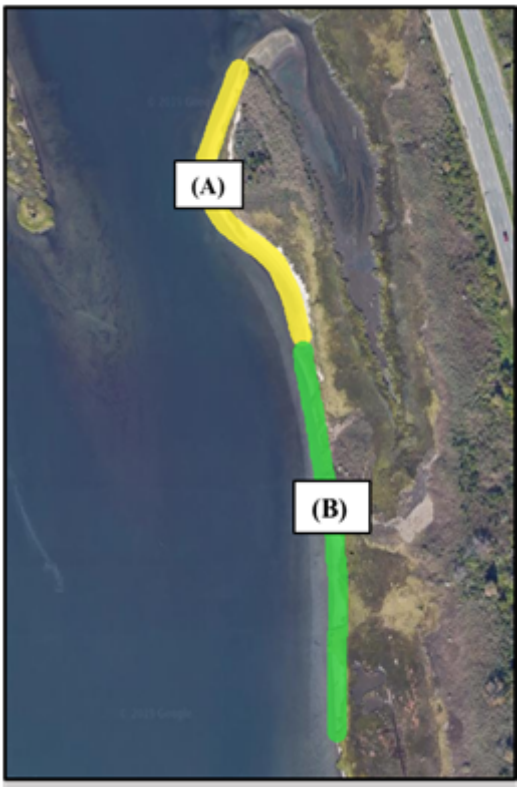

Site 6	FREEPORT CREEK ROCKY BEACH SIDE 1 (A)		
Location	Loss (g)	Loss (%)	MT Rate (g/hr)
L1	13.95	19.65	0.29
L2	15.55	21.90	0.32
L3	20.54	28.93	0.43
L4	19.34	27.24	0.40
L5	15.77	22.21	0.33
Average	17.03	23.99	0.35

Site 5	FREEPORT CREEK ROCKY BEACH SIDE 2 (B)		
Location	Loss (g)	Loss (%)	MT Rate (g/hr)
L1	23.90	33.66	0.50
L2	23.67	29.71	0.49
L3	29.92	30.89	0.62
L4	25.63	36.10	0.53
L5	33.07	42.49	0.69
Average	27.24	34.57	0.57

Figure 7

Environmental Energetics of Location 1: Freeport Creek (Top) Figure 7: Freeport Creek Rocky Beach. Freeport Creek Rocky Beach comprised 2 out of the 5 total sites for the Freeport Creek study location. The highlighted sections (A) and (B) with the following identically labeled tables. (Bottom) Table 2: Mass-Transfer Rates of Freeport Creek Island. Mass-transfer rates were gathered at 5 evenly distanced points along each 150-meter-long transect, labeled L1-L5 within each site.

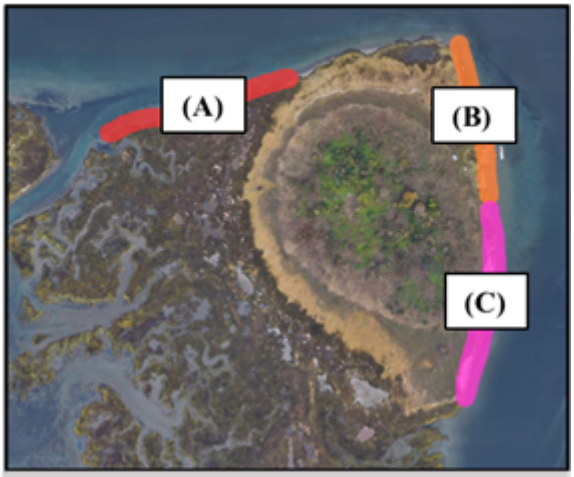

Site 1	SMITH MEADOW NORTH SIDE			(A)
Location	Loss (g)	Loss (%)	MT Rate (g/hr)	
L1	18.31	25.79	0.38	
L2	21.60	20.89	0.45	
L3	23.17	32.63	0.48	
L4	19.71	21.25	0.41	
L5	-9.19	-12.94	-0.19	
Average	14.72	17.52	0.31	
Site 2	SMITH MEADOW EAST SIDE 1			(B)
Location	Loss (g)	Loss (%)	MT Rate (g/hr)	
L1	23.72	26.23	0.49	
L2	5.29	7.06	0.11	
L3	32.36	30.09	0.67	
L4	30.64	33.10	0.64	
L5	29.23	29.08	0.61	
Average	24.25	25.11	0.51	
Site 9	SMITH MEADOW EAST SIDE 2			(C)
Location	Loss (g)	Loss (%)	MT Rate (g/hr)	
L1	23.89	33.65	0.50	
L2	23.42	32.99	0.49	
L3	22.44	31.61	0.47	
L4	23.63	33.28	0.49	
L5	30.77	31.98	0.64	
Average	24.83	32.70	0.52	

Figure 8

Environmental Energetics of Location 2: Smith Meadow (Top) Figure 8: Smith Meadow. Smith Meadow comprised 3 of the 5 total sites for the Smith Meadow location. The highlighted sections (A), (B), and (C) correspond with the following identically labeled tables. (Bottom) Table 3: Mass-Transfer Rates of Smith Meadow. Mass-transfer rates were gathered at 5 evenly distanced points along each 150-meter-long transect, labeled as L1-L5 within each site.

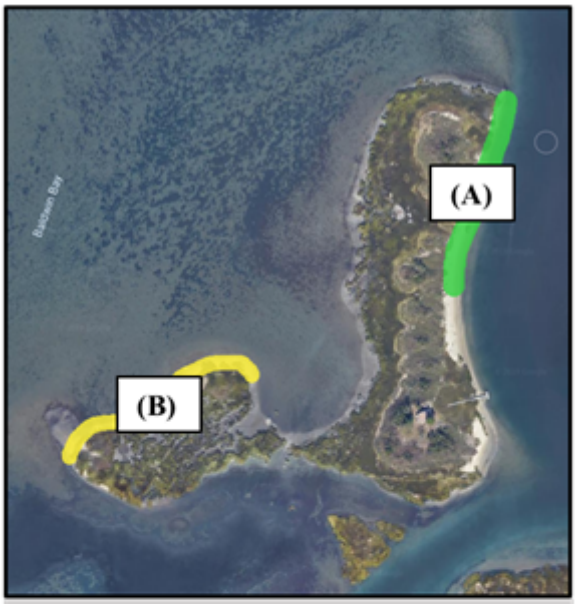

Site 10	SMITH MEADOW ISLAND FRONT SIDE			(A)
Location	Loss (g)	Loss (%)	MT Rate (g/hr)	
L1	38.63	42.74	0.80	
L2	29.82	42.00	0.62	
L3	43.81	47.69	0.91	
L4	28.76	29.48	0.60	
L5	42.73	42.00	0.89	
Average	36.75	40.78	0.77	
Site 3	SMITH MEADOW ISLAND BACK SIDE			(B)
Location	Loss (g)	Loss (%)	MT Rate (g/hr)	
L1	-7.61	-7.67	-0.16	
L2	-5.02	-5.57	-0.10	
L3	-6.55	-5.90	-0.14	
L4	-6.03	-6.77	-0.13	
L5	-6.34	-6.33	-0.13	
Average	-6.31	-6.45	-0.13	

Figure 9

Environmental Energetics of Location 2: Smith Meadow (Top) Figure 9: Smith Meadow Island. Smith Meadow Island comprised 2 of the 5 total sites for the Smith Meadow study location. The highlighted sections (A) and (B) correspond with the following identically labeled tables. (Bottom) Table 4: Mass-Transfer Rates of Smith Meadow Island. Mass-transfer rates were gathered at 5 evenly distanced points along each 150-meter-long transect, labeled as L1-L5 within each site.

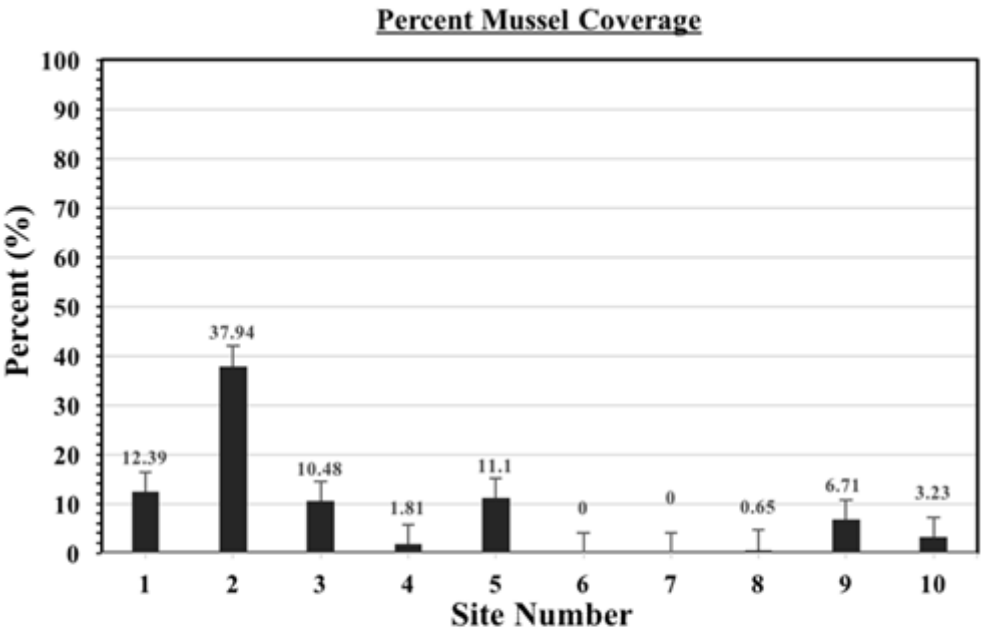

PERCENT MUSSEL COVER

Quadrat	Site 1	Site 2	Site 3	Site 4	Site 5	Site 6	Site 7	Site 8	Site 9	Site 10
Q1	16.00	56.00	0.00	0.00	0.00	0.00	0.00	0.00	0.00	0.00
Q2	28.00	0.00	76.00	0.00	76.00	0.00	0.00	0.00	0.00	0.00
Q3	20.00	40.00	0.00	0.00	80.00	0.00	0.00	0.00	0.00	0.00
Q4	8.00	0.00	32.00	0.00	0.00	0.00	0.00	0.00	0.00	0.00
Q5	4.00	36.00	0.00	0.00	0.00	0.00	0.00	0.00	0.00	0.00
Q6	12.00	24.00	0.00	0.00	0.00	0.00	0.00	0.00	0.00	0.00
Q7	8.00	28.00	0.00	0.00	0.00	0.00	0.00	0.00	0.00	0.00
Q8	4.00	28.00	52.00	0.00	0.00	0.00	0.00	0.00	0.00	0.00
Q9	8.00	4.00	0.00	0.00	0.00	0.00	0.00	0.00	0.00	100.00
Q10	4.00	16.00	88.00	0.00	0.00	0.00	0.00	0.00	0.00	0.00
Q11	0.00	28.00	76.00	0.00	56.00	0.00	0.00	0.00	28.00	0.00
Q12	8.00	52.00	0.00	0.00	0.00	0.00	0.00	0.00	0.00	0.00
Q13	0.00	12.00	0.00	0.00	0.00	0.00	0.00	0.00	40.00	0.00
Q14	0.00	68.00	0.00	0.00	0.00	0.00	0.00	0.00	0.00	0.00
Q15	20.00	28.00	0.00	0.00	0.00	0.00	0.00	0.00	72.00	0.00
Q16	4.00	76.00	0.00	0.00	36.00	0.00	0.00	0.00	68.00	0.00
Q17	28.00	60.00	0.00	0.00	0.00	0.00	0.00	0.00	0.00	0.00
Q18	8.00	56.00	0.00	0.00	0.00	0.00	0.00	0.00	0.00	0.00
Q19	28.00	12.00	0.00	0.00	16.00	0.00	0.00	0.00	0.00	0.00
Q20	0.00	52.00	0.00	0.00	0.00	0.00	0.00	0.00	0.00	0.00
Q21	16.00	0.00	0.00	56.00	0.00	0.00	0.00	0.00	0.00	0.00
Q22	16.00	84.00	0.00	0.00	80.00	0.00	0.00	0.00	0.00	0.00
Q23	0.00	64.00	0.00	0.00	0.00	0.00	0.00	0.00	0.00	0.00
Q24	4.00	32.00	0.00	0.00	0.00	0.00	0.00	0.00	0.00	0.00
Q25	4.00	28.00	0.00	0.00	0.00	0.00	0.00	0.00	0.00	0.00
Q26	72.00	56.00	0.00	0.00	0.00	0.00	0.00	0.00	0.00	0.00
Q27	0.00	84.00	0.00	0.00	0.00	0.00	0.00	0.00	0.00	0.00
Q28	12.00	56.00	0.00	0.00	0.00	0.00	0.00	0.00	0.00	0.00
Q29	0.00	0.00	0.00	0.00	0.00	0.00	0.00	0.00	0.00	0.00
Q30	24.00	96.00	0.00	0.00	0.00	0.00	0.00	0.00	0.00	0.00
Q31	28.00	0.00	0.00	0.00	0.00	0.00	0.00	20.00	0.00	0.00
Average	12.39	37.94	10.45	1.81	11.10	0.00	0.00	0.65	6.71	3.23

Figure 10

Mussel Coverage Assessment (Top) Figure 10: Percent Mussel Coverage. Average mussel coverage was assayed via quadrat measurements, with the average of each site shown in the graph above. Error bars represent the average percent variance within each sites collection, roughly 4% for each coverage for each bar. (Bottom) Table 5: Percent Mussel Coverage. Mussel coverage was measured in the field. Averages coverage for each site was calculated (last row of table) from 31 quadrat measurements, represented as Q1-Q31.

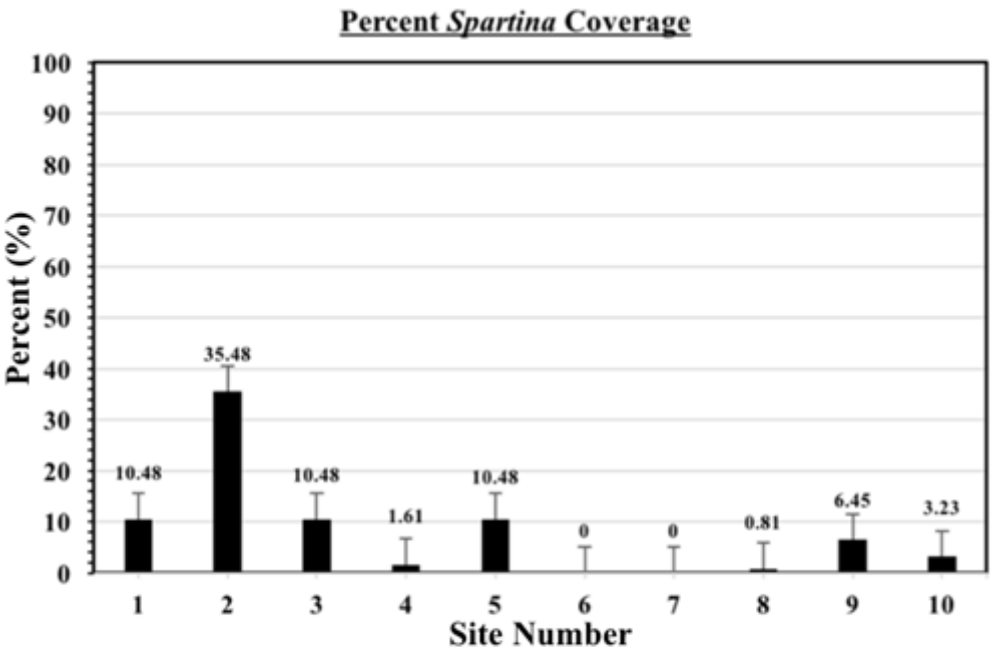

PERCENT *SPARTINA* COVER

Quadrat	Site 1	Site 2	Site 3	Site 4	Site 5	Site 6	Site 7	Site 8	Site 9	Site 10
Q1	25.00	50.00	0.00	0.00	0.00	0.00	0.00	0.00	0.00	0.00
Q2	25.00	0.00	75.00	0.00	75.00	0.00	0.00	0.00	0.00	0.00
Q3	25.00	50.00	0.00	0.00	75.00	0.00	0.00	0.00	0.00	0.00
Q4	0.00	0.00	25.00	0.00	0.00	0.00	0.00	0.00	0.00	0.00
Q5	0.00	25.00	0.00	0.00	0.00	0.00	0.00	0.00	0.00	0.00
Q6	0.00	25.00	0.00	0.00	0.00	0.00	0.00	0.00	0.00	0.00
Q7	0.00	25.00	0.00	0.00	0.00	0.00	0.00	0.00	0.00	0.00
Q8	0.00	25.00	50.00	0.00	0.00	0.00	0.00	0.00	0.00	0.00
Q9	0.00	0.00	0.00	0.00	0.00	0.00	0.00	0.00	0.00	100.00
Q10	0.00	25.00	100.00	0.00	0.00	0.00	0.00	0.00	0.00	0.00
Q11	0.00	25.00	75.00	0.00	50.00	0.00	0.00	0.00	25.00	0.00
Q12	0.00	25.00	0.00	0.00	0.00	0.00	0.00	0.00	0.00	0.00
Q13	0.00	0.00	0.00	0.00	0.00	0.00	0.00	0.00	25.00	0.00
Q14	0.00	75.00	0.00	0.00	0.00	0.00	0.00	0.00	0.00	0.00
Q15	25.00	25.00	0.00	0.00	0.00	0.00	0.00	0.00	75.00	0.00
Q16	0.00	75.00	0.00	0.00	25.00	0.00	0.00	0.00	75.00	0.00
Q17	25.00	75.00	0.00	0.00	0.00	0.00	0.00	0.00	0.00	0.00
Q18	0.00	50.00	0.00	0.00	0.00	0.00	0.00	0.00	0.00	0.00
Q19	25.00	0.00	0.00	0.00	25.00	0.00	0.00	0.00	0.00	0.00
Q20	0.00	50.00	0.00	0.00	0.00	0.00	0.00	0.00	0.00	0.00
Q21	25.00	0.00	0.00	50.00	0.00	0.00	0.00	0.00	0.00	0.00
Q22	25.00	75.00	0.00	0.00	75.00	0.00	0.00	0.00	0.00	0.00
Q23	0.00	75.00	0.00	0.00	0.00	0.00	0.00	0.00	0.00	0.00
Q24	0.00	25.00	0.00	0.00	0.00	0.00	0.00	0.00	0.00	0.00
Q25	0.00	25.00	0.00	0.00	0.00	0.00	0.00	0.00	0.00	0.00
Q26	75.00	50.00	0.00	0.00	0.00	0.00	0.00	0.00	0.00	0.00
Q27	0.00	75.00	0.00	0.00	0.00	0.00	0.00	0.00	0.00	0.00
Q28	0.00	50.00	0.00	0.00	0.00	0.00	0.00	0.00	0.00	0.00
Q29	0.00	0.00	0.00	0.00	0.00	0.00	0.00	0.00	0.00	0.00
Q30	25.00	100.00	0.00	0.00	0.00	0.00	0.00	0.00	0.00	0.00
Q31	25.00	0.00	0.00	0.00	0.00	0.00	0.00	25.00	0.00	0.00
Average	10.48	35.48	10.48	1.61	10.48	0.00	0.00	0.81	6.45	3.23

Figure 11

Spartina Coverage Assessment (Top) Figure 11: Percent Spartina Coverage. Average percent Spartina coverage was assayed via quadrat measurements, with the average of each site shown above. Error bars represent the average percent variance within each sites collection, roughly 4% for each coverage for each bar. (Bottom) Table 6: Percent Spartina Coverage. Spartina coverage was measured in the field. Average coverage for each site was calculated (last row of table) from 31 quadrat measurements, represented as Q1-Q31.